Dynamical heterogeneity in nanoconfined poly(styrene) chains

D. B. Zax,[a] D.-K. Yang, R. A. Santos, and H. Hegemann
Cornell Center for Materials Research and Department of Chemistry and Chemical Biology, Cornell University, Ithaca, New York 14853

E. P. Giannelis and E. Manias[b]
Cornell Center for Materials Research and Department of Materials Science and Engineering, Cornell University, Ithaca, New York 14853

Fluids in nanoscopic confinements possess a variety of unusual properties, and in particular, remarkable dynamical heterogeneities which vary on length scales as short as a fraction of a nanometer. While the surface forces apparatus provides an experimental probe of macroscopic properties of fluids in contact with atomically smooth solid surfaces, few experimental probes are available which test the microscopic origins of these heterogeneities. In this article we describe our recent efforts to apply nuclear magnetic resonance spectroscopy to nanoscopically confined poly(styrene) (PS) created by intercalation into a surface-modified fluorohectorite. A comparison between surface-sensitive cross polarization experiments with spin–echo experiments which probe the entire organic layer suggests that PS in the center of the nanopores is more mobile than the bulk at comparable temperatures, while chain segments which interact with the surface are dynamically inhibited. © *2000 American Institute of Physics.* [S0021-9606(00)71206-2]

I. INTRODUCTION

Existing experimental studies of nanoscale systems, whether oligomeric or polymeric, and their interaction with atomically smooth solid surfaces, report remarkable changes in the dynamical properties of confined chains.[1–6] Both recent experimental results, and simulations, suggest that a wide range of dynamic modes are accessible to these confined molecules, and the distance from the confining surface appears to be a critical parameter in understanding those allowed dynamical modes. In this study, we present our initial efforts at providing a direct microscopic measure of segmental dynamics observed for a long polymer confined in a 2 nm slit pore between solid surfaces. Our experimental probe for these studies is solid state nuclear magnetic resonance (NMR) spectroscopy, and the experiments we describe probe chain dynamics in the gap. Remarkably, in these confined thin poly(styrene) (PS) layers we infer that the entire range of microscopic dynamical timescales describing local reorientational modes, ranging from slower to much faster than in bulk PS, are found simultaneously within a single slit pore. These experimental observations are clarified with reference to molecular dynamics (MD) simulations, which reveal striking density variations across the thin organic layers.

Recent surface forces apparatus (SFA)[7] experiments on fluid/solid interfaces in nanoscopic confinement report that where films are thinner than five monomer diameters, no flow is observed under shear. Instead, these thin films exhibit a solid-like response with a finite yield stress,[3,4,8] and the effective viscosity measured is two to three orders of magnitude higher than in bulk. At shear rates where the bulk liquids are still Newtonian, these films exhibit strong shear thinning.[5,6] Under the stress of pressure-induced changes in the distance between confining surfaces, SFA experiments show strongly quantized (layer-by-layer) film drainage, as well as wildly oscillating solvation forces, in both nanoscopically confined simple[9,10] and polymeric[11] systems. While the SFA measurements suggest that at least some microscopic processes of molecular relaxation are very slow—both for short oligomers and long polymers—these relaxation modes cannot be directly observed by the SFA.

In parallel with the SFA experiments, MD computer simulations have been used so as to clarify the microscopic modes associated with the SFA experimental, phenomenological observations of macroscopic properties.[12–17] In these simulations, characteristic time scales associated with segmental dynamics vary dramatically—over distances even as short as a single monomer diameter—in the immediate vicinity of a strongly physisorbing surface. Simulations of alkane chains in contact with confining surfaces further suggest[12,13] that the correlation times associated with *trans–gauche* isomerization vary by up to three orders of magnitude inside a single slit pore, and that the transition to bulk-like relaxation times occurs in the second layer of adsorbate—which may be as few as 0.5 nm from the surface. Thus the entire slow-down is observed *only* in the *immediate* vicinity (first layer) of an attractive surface,[12] while bulk behavior is recovered as quickly as in the next layer.

Although one might suspect that the inevitable epitaxial ordering found atop of atomically smooth surface could account for this behavior, computer simulations[14] suggest that density inhomogeneities normal to the confining surfaces—and, in particular, the densification of the fluid in the few angstroms most closely associated with the surface—are re-
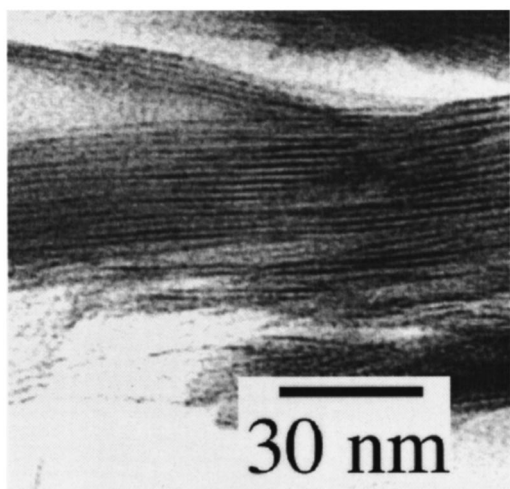
FIG. 1. Bright field TEM image of the structure of PS/C$_{18}$FH nanocomposites.

sponsible for the slow dynamics. Moreover, the energetics of polymer adsorption to the surface determine the degree of polymer densification, and therefore play a key role in determining the magnitude of the change in dynamics.[14] In support of these conclusions, experimental studies by Wallace *et al.*[18] have shown that strong attractive interactions (as between a hydrogen-terminated Si surface and PS) increase T_g near a surface, while less attractive interactions reduce T_g (as between their ''untreated'' Si surfaces and PS).

In this study we look to probe the dynamic time scales accessible to a 2 nm thin layer of high molecular weight poly(styrene) confined between the surfaces of layered fluorohectorite (FH).[19] Our experimental tools include ^{1}H–^{29}Si CPMAS and ^{2}H NMR. The former helps identify the oligomeric surface layer, while the latter provides a broad range of sensitivity to dynamical time scales. The combination allows to identify the slowest moving portion of the sample—which is, unsurprisingly, the surface layer—and to observe experimentally the surprising dynamical heterogeneity found on extremely short length scales.

II. SAMPLE PREPARATION

FH (Ref. 20) is a synthetic phyllosilicate with typical lateral dimensions of 3–7 μm, and a layer thickness of 1 nm. The surfaces are modified by ion exchange with alkyl-ammonium cationic surfactants ($C_{18}H_{37}NH_3^+$). The surfactant grafting density, which is characteristic of the specific silicate and its charge density, is approximately 1.12/nm^2. PS is intercalated between the silicate surfaces, and the two-dimensional inorganic platelets self-assemble into parallel sheets separated by an organic film 2 nm thick (see Fig. 1). While other silicates are popular hosts for polymer intercalation,[19] for these studies FH possesses one significant advantage. As a synthetic material, its chemical purity is determined by the synthetic procedure and there is no measurable content of Fe^{3+}. NMR spectra observed in these systems are therefore sensitive to local environment and dynamics.[21] Naturally occurring layered silicates, such as montmorillonite, often contain levels of paramagnetic impurities sufficient to dominate the observable NMR features.[22]

Samples were prepared via melt polymer intercalation of PS into an octadecyl-ammonium modified fluorohectorite, as has previously been described.[23] Polymer dynamics can be studied by ^{2}H solid state NMR, and selectively labeled samples were therefore prepared: in the first, a commercially supplied PS derived from d-3 styrene was intercalated. A second sample was prepared similarly except for the use of d-5 styrene. This afforded us the ability to focus individually on dynamic modes either at the aliphatic backbone, or at the phenyl sidechains. (Due to the relative insensitivity of the deuterium quadrupole coupling to fine chemical details, however, it was not possible to separate out the dynamics of methine from methylene sites along the backbone, or the ortho, meta, or para sites on the phenyl group. Such experiments would, in general, require samples specifically labeled at each individual site.) In addition, a separate series of samples were prepared where the organically modified silicates were ion exchanged with deuterated ammonium groups ($C_{18}H_{37}ND_3^+$) and subsequently intercalated PS derived from either d-3, d-5, or d-8 (perdeuterated) styrene. These samples were used to study polymer interactions between the remaining ^{1}H atoms and the silicate surface.

The presence of well-ordered multilayers was confirmed by x-ray diffraction. Diffraction measurements can be combined with thermal gravimetric analysis (TGA)—which provides the organic-to-inorganic mass ratio—and confirm that the polymer exists essentially only inside the interlayer galleries. The intercalated organic material consists of 68 wt % polymer and 32 wt % $C_{18}H_{37}NH_3^+$ in typical PS/C$_{18}$–FH nanocomposites. These weight fractions are in very good agreement with the TGA results of PS/C$_{18}$–FH samples intercalated *at capacity,* i.e., all silicate interlayers are swollen by polymer, and there is no residual free polymer.

III. MOLECULAR MODELING

While the full power of MD is most often used to probe dynamical properties—and such a study is currently underway—the limited time scales simulated to date in our MD studies are of little use in understanding the NMR experiments which follow in this article. On the other hand, Monte Carlo (MC) simulations of PS intercalated into surface modified FH can be used to provide a detailed picture of the structure of the polymer confined in the interlayer gallery of the FH host. As details of the simulations are given elsewhere,[24] here we make only brief mention of the techniques employed.

The rotational-isomeric-state model was used to create initial polymer conformations of PS.[25] Conformations that fit in the interlayer gallery were chosen, and equilibrated with MC schemes in coexistence with the grafted surfactant molecules. Numbers of polymer chains and alkyl-ammonium surfactants were chosen so as to match the densities found in the experimental studies (see sample preparation). Several MC equilibrated system configurations were subsequently used as initial systems for relatively short (1–10 ns) MD runs. While several force fields have been proposed for PS,[26]
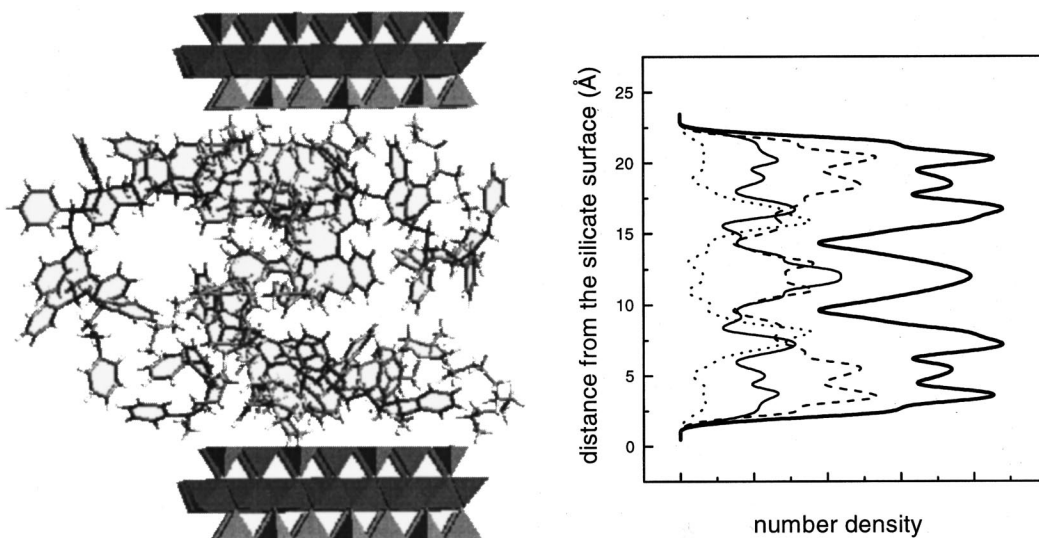
FIG. 2. (Left) Simulation snapshot from MD simulation of silicate–surfactant–PS nanocomposite system, which gives an atomistic picture of the various system components. (Right) The corresponding, ensemble averaged, number density of carbon atoms as a function of distance offset from the lower confining silicate surface. The dotted line corresponds to the polymer backbone, the dashed to the polymer phenyls, the thin solid line to the alkyl-ammonium surfactant, and the thicker solid line to the total.

the force field of Müller-Plathe[27] was chosen, because when combined with the force field we have developed for the organo-silicates,[28] it reproduces the experimentally observed d spacings found in the PS/C_{18}FH nanocomposites. After equilibration of the initial system configuration, the gallery structure is obtained—a snapshot of which is shown in Fig. 2. A more concise representation is provided by a plot of the various atomic probability distribution functions shown in the carbon-atom density profiles of Fig. 2. The density profiles clearly demonstrate that the organic phase in the galleries (comprised of both the polymer and the tethered alkyl chains) organizes in three layers. Moreover, within each of the three layers, the carbon-atom distributions are even more finely layered, due to the combined constraints of chain connectivity and packing efficiency.

Focusing momentarily only on the polymer configuration provides some clues as to the origin of this layering effect. We find that the polymer backbone is predominately located near the confining wall—and at distances of about 0.3–0.7 nm from that wall—but more removed, on average, than most of the phenyl sidechains. Often, a short strand of polymer adopts a bridging configuration perpendicular to, and connecting between, both walls. The phenyl rings, which attach to the backbone at each methine, are similarly found in all three layers but are predominantly nearest the silicate surface. Finally, while surfactant methylenes are found distributed in all three layers, they bunch preferentially in the middle layer. As the head group of the surfactant is tethered via an ionic interaction to the negatively charged silicate, it cannot be completely displaced from the surface. In contrast, PS does displace the surfactant's aliphatic chains, and preferentially interacts with the surface, in agreement with mean field theory predictions by Vaia and Giannelis.[29]

IV. EXPERIMENTAL APPROACHES BASED ON NMR

A. Surface layer structure: ^{1}H–^{29}Si double resonance NMR spectroscopy

The precise balance of forces between the various interactions remains a question of some importance. In these multicomponent systems, we have a surface-specific probe due to the existence of ^{29}Si, a naturally occurring dilute spin label (roughly 4.7% of the Si sites) with good receptivity in NMR experiments. Only a single Si chemical environment is observed under high-resolution conditions—i.e., magic angle spinning (MAS) combined with high-power ^{1}H decoupling—indicating that the organic molecules in the galleries interact too weakly with the electronic structure of the silicate lattice to generate resolvable chemical shifts.

As the fluorohectorite lattice contains no ^{1}H atoms, relative strengths of the different organic/inorganic interactions can be probed by a double resonance experiment, where chemical selectivity is achieved by the use of selective isotopic labels. We observe the MAS ^{29}Si NMR signal only after magnetization has been transferred via a variable time period of cross polarization (CP) from nearby ^{1}H spins. CP intensity curves are generally modeled using a three parameter fit[30]

$$I_{^{29}\text{Si}}(\tau_{\text{CP}}) = \frac{M_{\text{CP}}}{1-\lambda}(1 - e^{-(1-\lambda)\tau_{\text{CP}}/T_{\text{H–Si}}})e^{-\tau_{\text{CP}}/T_{1\rho}^{\text{H}}}, \quad (1)$$

where

$$\lambda = \frac{T_{\text{H—Si}}}{T_{1\rho}^{\text{H}}}.$$

Thus a polarization transfer experiment involves measuring the amplitude of the ^{29}Si NMR signal as a function of the

a)   Cross polarization
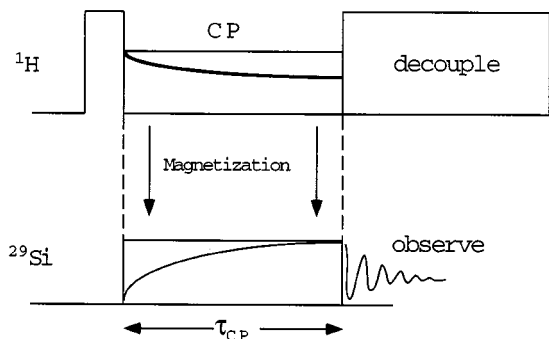
b)   Quadrupolar Echo
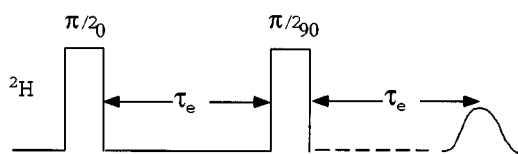
FIG. 3. NMR experiments used in this work to probe polymer structure and dynamics. (a). Cross polarization experiment for pairs of $I = \frac{1}{2}$ spins (i.e., ^{1}H and ^{29}Si). During the cross polarization period magnetization is transferred from ^{1}H sites to nearby ^{29}Si sites. The rate of magnetization transfer decreases with increased distance and/or dynamics. (b). Quadrupole spin–echo experiment for $I = 1$ (i.e., ^{2}H). A pair of 90° pulses, of phases differing by $\pi/2$, are applied τ μs apart. A spin echo of intensity equal to that of the signal after the first pulse is observed if there is no dynamics on time scales comparable to τ.

length of the CP period, τ_{CP}, as illustrated in Fig. 3(a). Each such experimental curve is fit to a set of three parameters M_{CP}, $1/T_{H-Si}$, and $1/T_{1\rho}^{H}$. Theories based on simplified models of the CP dynamics predict CP signals enhanced in magnitude (by comparison to the equilibrium signal associated with the ^{29}Si nuclei) in the amount $|\gamma_H/\gamma_{Si}| \approx 5$.[30] More sophisticated theory,[31] and experimental practice, suggests that for CP experiments where only a small number of nearby ^{1}H sites contributes, enhancements are only 60%–75% as large.

M_{CP} measures the number of ^{29}Si sites in proximity to ^{1}H magnetization sources, the experimentally achieved CP enhancement factor and various instrumental parameters. The rate of signal intensity recovery, $1/T_{H-Si}$, depends on the shortest ^{1}H–^{29}Si distances. Modes of ^{1}H magnetization loss are collectively described by the rate of magnetization dephasing, $1/T_{1\rho}^{H}$. In the nanocomposites, the dephasing processes limit the useful range of magnetization transfer distances to less than 0.5 nm, so that ^{29}Si in the silicate can be observed when a ^{1}H from only the closest of the three organic layers (see Fig. 2) remains in close proximity for the few milliseconds required to effect CP.

In CP experiments on the nanocomposite samples the charged head groups ($-$N^{1}H$_3$) of the alkyl-ammonium surfactants normally dominate the magnetization transfer to the silicate surface, as they are found at the shortest Si–H distances and are immobile. So as to focus more directly on the

untethered groups, we prepared a surface-modified silicate with ^{2}H atoms incorporated into the head group by exchange in acid solution. Under these conditions, the nearest ^{1}H sites on the cation are at the α-CH$_2$, at distances comparable to the closest hydrogen atoms found in PS near the surface (see Fig. 2).

B. Polymer dynamics: ^{2}H NMR spectroscopy

Polymer dynamics can be probed most effectively via ^{2}H NMR experiments.[32–34] A class of particularly simple experiments is to monitor the intensity of a signal as a function of temperature, as in the spin–echo experiment shown in Fig. 3(b). In modern time-domain NMR experiments spin echoes are frequently required so that weak NMR signals can be observed far removed from the high-power excitation pulses. In a quadrupolar spin–echo experiment as illustrated, complete refocusing of the signal at a time $2\tau_e$ can be achieved, as long as there is no change in resonance frequency in the time periods before and after the second pulse. Where there is a significant change in frequency on a time scale comparable to τ_e, however, signals from such sites are lost due to incomplete refocusing (which relies on the "reversal" of the direction of spin evolution without change in evolution frequency, i.e., at identical orientation).

Under the conditions typically associated with a quadrupolar echo in ^{2}H NMR, the orientation-dependent resonance frequency is determined by the direction of the C–H bond with respect to the externally applied magnetic field, thus signal intensity loss is a marker of large-amplitude dynamics. For the PS backbone, these modes should correspond to *trans–gauche* isomerization and/or translation; for the phenyl groups, some combination of ring flips and translation. In their study of PS/toluene glasses, Rossler *et al.*[35] showed that the sudden shortening in the T_2 parameter characterizing refocusing in a quadrupolar echo—to a value of order 200 μs for polymer-rich preparations—could be used as a marker for T_g.

V. EXPERIMENTAL RESULTS

A. Structure of the surface layer

In traditional high-resolution NMR studies of ^{1}H spins, each spin generates a spectroscopic signature with the same intensity. In solid state samples, this simple relationship between numbers of spins and signal intensities can be approximated by observation of signal intensities in the simplest NMR experiment, the Bloch decay (without enhancement from, e.g., CP) and, where signal averaging is required, at very long delays between successive scans. Such quantitatively accurate experiments are thus quite time consuming, and executed only when necessary. By contrast, CP intensities measure—to within an experimental constant somewhat smaller than one—the number of Si sites near to ^{1}H nuclear spins. Where we wish to compare CP signal intensities between samples and thereby learn about surface coverage, both experiments are necessary. Thus for each sample (d-3, d-5, or d-8 PS) the Bloch decay intensities were measured at 300 K and at different pulse repetition rates. The measured signal intensities were extrapolated to infinite time between

J. Chem. Phys., Vol. 112, No. 6, 8 February 2000

Nanoconfined poly(styrene) chains   2949
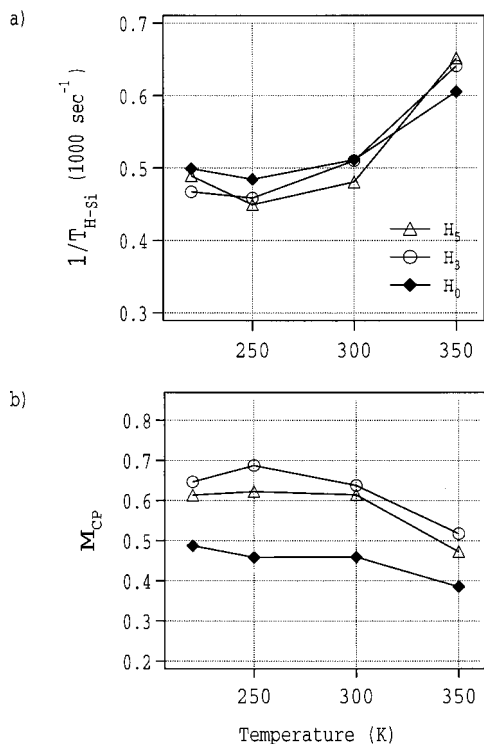
FIG. 4. ^{29}Si CP rates and intensities, as a function of T and sample, observed in the surface-modified FH samples with a labeled PS intercalates. At low T, rates and intensities are largely independent of T. Both d-3 and d-5 PS yield more ^{29}Si signal than is observed in d-8 PS, indicating that the PS is in close proximity to the silicate surface. At 350 K, all intensities decrease—because mobile styrene no longer sources magnetization—and rates increase—because the more mobile components are also further from the surface.

successive scans so as to account for the long ^{29}Si spin–lattice relaxations times, T_1, and the result was the Si spin count for that sample. CP-enhanced signal intensities were then divided by the Si spin count and the nominal CP-enhancement factor (5) (and corrected for the natural variation in spin signal intensity with $1/T$ at temperatures other than 300 K). The values resulting from this process are described in Fig. 4, where the corrected CP signal intensities M_{CP}, and transfer rates $1/T_{H-Si}$, calculated by fitting to Eq. (1), are shown.

In the d-8 PS nanocomposite, the ^{29}Si signal M_{CP} is 0.47 of its theoretical maximum. Both the intensity and the rise time—a rough indication of mean ^{1}H–^{29}Si distance—remain essentially unchanged for 200 K $< T <$ 300 K. Where ^{1}H is found in the backbone (d-5 PS) or on the phenyl rings (d-3 PS) as well as in the aliphatic surfactant chain, the CP fraction reaches 0.67 and 0.62, respectively, indicating that essentially all the surface Si sites are within the sphere of influence of a ^{1}H in one of the organic constituents of the intergallery layer. The increase in CP fraction reflects the proximity of the polymer to the silicate surface. Cross relaxation rates $1/T_{H-Si}$ differ only minimally from those observed in the perdeuterated nanocomposite.

In contrast, measurements at 350 K show significant intensity losses in each of the three samples, with M_{CP} ranging from 0.39 in the perdeuterated PS sample, to 0.47 (d-3) and 0.51 (d-5) in the samples containing partially protonated PS. Simultaneously, the cross-relaxation rate *increases*, indicat-
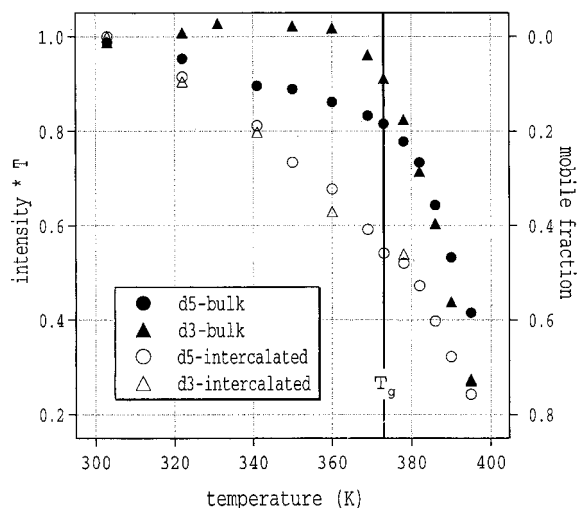
FIG. 5. Intensities (multiplied by T, which corrects for the Curie temperature decrease of observable intensity with increased T) observed in ^{2}H quadrupole spin–echo experiments, for d-3 and d-5 PS, in bulk and intercalated in surface-modified FH. Intensities less than one correspond to ^{2}H sites mobile on the time scale of the spin echo experiment, as is indicated in the right-hand axis system. In bulk, ring modes are enabled somewhat below T_g, while backbone modes become significant only near T_g. In intercalated samples, the two modes are coupled and grow in over a broad temperature range from well below T_g, suggesting the existence of faster modes in confined PS than are found in bulk PS.

ing that the ^{1}H sites available to transfer polarization are *closer* on average than at lower T—and that the average distance ^{1}H–^{29}Si is virtually identical in all the measured samples. This would suggest that at this elevated temperature elements of the organic interlayer even within the first layer have very different dynamics. Immediately atop the surface the ^{1}H sites available to transfer magnetization move little, while those ^{1}H atoms only minimally removed from the surface are no longer capable of transferring magnetization during the CP process. *This clearly identifies the slowest-moving styrene moieties as the surface-adsorbed species.*

B. Dynamics of intergallery PS

Figure 5 shows our evidence for very heterogeneous dynamics in the polymer component of the nanocomposites over the entire 2 nm film thickness. In Fig. 5 we show the spectral intensity (integrated over the entire relevant bandwidth) observed in quadrupolar-echo spectra[36] with echo spacings $\tau = 20$ μs for d-5 and d-3 PS, in bulk and in the nanocomposite. Raw integrated signal amplitudes are scaled by temperature so as to correct for the natural decrease in NMR signal amplitude with increasing temperature; for each of the four samples the nominal intensity has been normalized to unity at the $T = 303$ K. (Below this temperature individual data points are too costly to obtain due to exceedingly long T_1 values.)

Two very different types of signals are identified in each of the four samples—the observable signals arising from sites with long T_2 and slow (millisecond and longer time scale) dynamics, and the unobserved signals associated with short T_2's and more rapid (microseconds) dynamics. Following Rössler,[35] who demonstrated that in PS–toluene mixtures

the onset of the glassy phase could be identified by T_2 < 100 μs, we assign the more mobile (and invisible) portions of the sample to a phase with glass-like dynamics. (Additionally, a quite small fraction of the observed signal in the intercalated ring sites is averaged in a fashion which suggests the possibility of the rapid, large-amplitude flips.) At all temperatures, line shapes observed for the slowly reorienting sites, both in bulk and intercalated samples, are similar to the traditional Pake powder patterns associated with static C–H bonds, and so the one-dimensional line shape information appears to contain little information about dynamics. Instead, it is the signal intensities, only, which allow us to characterize dynamics.

In bulk PS samples there is a dramatic difference between the temperature dependences of the intensities observed for the backbone- and ring-labeled samples. Below the bulk value of T_g, only the deuterons in the ring-labeled (d-5) PS undergo significant dynamics, due to the availability of large-amplitude rocking modes of the rings. Significant signal loss at the backbone sites, however, is observed only in the temperature region $T > T_g$. Thus, the magnitude of the ''missing'' signal in the spectra of the bulk PS (d-3) sample is in direct proportion to the fraction of styrene moieties which are ''glassy,'' i.e., whose dynamic modes are active on a time scale comparable to the time between pulses.

Figure 5 also shows the measured intensities found for the same two PS samples intercalated into the organically modified fluorohectorite, where the polymer is ''confined.'' Over a very broad temperature range, and well below the bulk T_g, signal disappears from the ^{2}H quadrupole echo spectrum of the intercalated d-5 PS, and near the bulk T_g the missing signals are about twice as large as in the bulk. Unlike in bulk PS, the loss of signal intensity in the intercalated d-3 PS tracks that found in the d-5 PS, indicating that the accessible slow modes involve the entire polymer—so that the loss of signal intensity corresponds to a progressive increase in the fraction of mobile styrene units. Moreover, no discontinuities which might identify phase transitions are observed in the vicinity of the bulk T_g in the nanocomposites. This is in very good agreement with differential scanning calorimetry (DSC) studies of similarly prepared samples that show no evidence for a glass transition in the temperature range 293 K$<T<$473K, as shown in Fig. 6.

VI. COMPARISON TO BULK PS

Based on quadrupole spin echo intensities in selectively deuterated polystyrenes, it has previously been demonstrated that at room temperature (and thus well below $T_g \approx 373$ K) in bulk PS dynamics is quite limited. Motionally averaged line shapes are found at lowest temperatures in ^{2}H spectra of d-5 polystyrene, which reflect the ability of the PS sidechains to execute rapid flips through large angles even in the glassy phase of PS.[32] Similarly averaged line shapes in bulk d-3 PS, however, are observed only in the vicinity of T_g, suggesting that the dynamical modes at the two sites are effectively decoupled. Careful analysis of complementary ^{13}C NMR data at ambient temperature suggested that ring flips occur at
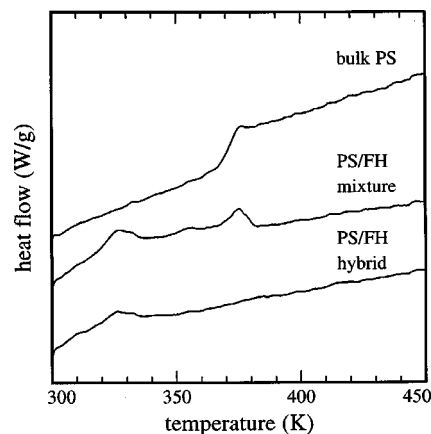
FIG. 6. DSC traces for 293 K$<T<$473 K for our PS-based nanocomposite, the pure constituent PS, and a physical mixture of surfactant-modified FH and bulk PS before intercalation. In bulk PS, T_g is observed at about 373 K; in the surface-modified silicate, transitions at about 330 and 360 K reflect ordering transitions of the alkyl ammonium surfactant. For the intercalated–confined–PS, no evidence of any polymer phase transitions is observed from well below the bulk T_g to well above.

rates ~ 10 MHz.[37] Both studies further suggested the existence of lower-amplitude ring modes at slower (i.e., kHz) rates.

In contrast, in toluene-plasticized PS the fraction of phenyl groups undergoing rapid ring flips is decreased[38] even as T_g is lowered, and both sidechain and backbone dynamics reflect the same microscopic modes.[35] While T_g decreases as the ratio of plasticizer to monomer increases, for any composition the phase transitions are observed in a narrow temperature range. This behavior is in sharp contrast to what is observed in the nanocomposites, where sidechain and backbones are coupled tightly, and spread throughout the sample over a transition region nearly 100 K wide.

VII. CONCLUSIONS

CP experiments are useful as they provide us with a measure of the local environment experienced by ^{29}Si nuclear spins trapped in the lattice. These experiments demonstrate that the organic layer directly atop the silicate surface includes PS, both phenyl and backbone groups. Styrene units sufficiently close to the surface to provide polarization for CP experiments seem to maintain their structure until at least 300 K. Above 350 K, the CP evidence suggests that while the layer in most immediate contact with the surface maintains its integrity, styrene moieties not in direct contact with the silicate surface either pull away, become more dynamic, or both. The MD computer simulations (on, of course, a vastly shorter time scale) show a similar dynamic gradient.

The ^{2}H NMR experiments are complementary to the CP experiments, in that they provide a polymer's-eye view of local environment. The quadrupole echo experiment indicates that phenyl group dynamics is intimately entangled with backbone dynamics. Furthermore, the transition between the glassy polymer and the melt takes place over an unusually broad temperature range. In companion T_1 relaxation studies, we further find that the distribution of reorien-

tation correlation times for PS in our nanocomposites are always both broader and entirely contain the corresponding distributions found in bulk PS. Neither in this system, nor in a Li/PEO/FH nanocomposite,[21] where T_m of the bulk PEO is $\sim$ 335 K and is easily exceeded, has a high-temperature isotropic phase been observed in these highly oriented two-dimensional intercalated polymers.

The combination of ^{2}H NMR spectroscopy and CP intensity measurements suggests that the dynamically slowest styrene moieties are found in the immediate vicinity of the silicate surface. Faster modes appear to be characteristic of the parts of the polymer chains located toward the center of the intercalated film, where the local density (see Fig. 2) is lower. This result would not appear to be in conflict with an increase in viscosity in thin confined films. As the polymer is held together by strong covalent bonds, macroscopic displacements—as are probed by viscosity measurements—are determined by the *slowest* moving segments of the polymer. Even where mobile styrene moieties are found in the center of an interlayer gap, where they are tethered by a small number of bonds to portions of the polymer ''frozen'' to the surface, then even the mobile units can undergo no large-scale displacements. Therefore, increases in viscosity need not be associated with uniform slowing down of the dynamics—as long as some portion of the sample in fact is slowed. These findings are in good agreement with recent experiments using dielectric spectroscopy as a probe of dynamics in confined polymer layers.[39] A new dynamical mode is observed in these confined oligomers which is only weakly temperature dependent, and is much faster than the α relaxation in bulk polymers. Where the polymer is not confined (i.e., in homogeneous blends of the surfactant and polymer) no corresponding mode is found.

ACKNOWLEDGMENTS

[1] A. M. Homola, H. Nguygen, and G. Hadziioannou, J. Chem. Phys. **94**, 2346 (1991).

[2] J. P. Montfort and G. Hadziioannou, J. Chem. Phys. **88**, 7187 (1988).

[3] M. L. Gee, P. M. McGuiggan, J. N. Israelachvili, and A. M. Homola, J. Chem. Phys. **93**, 1895 (1990).

[4] J. van Alsten and S. Granick, Macromolecules **23**, 4856 (1990).

[5] H. Hu, G. A. Carson, and S. Granick, Phys. Rev. Lett. **66**, 2758 (1991).

[6] G. Carson, H. Hu, and S. Granick, Tribol. Trans. **35**, 405 (1992).

[7] D. Tabor and R. H. Winterton, Proc. R. Soc. London, Ser. A **312**, 543 (1969); D. Tabor and J. N. Israelachvilli *ibid.* **331**, 19 (1972); J. N. Israelachvilli and G. E. Adams, J. Chem. Soc., Faraday Trans. 1 **74**, 975 (1978).

[8] J. Klein and E. Kumacheva, Science **269**, 816 (1995).

[9] D. Y. C. Chan and R. G. Horn, J. Chem. Phys. **83**, 5311 (1985).

[10] H. K. Christenson, J. Chem. Phys. **78**, 6906 (1983).

[11] R. G. Horn, S. J. Hirz, G. Hadziioannou, C. W. Frank, and J. M. Catala, J. Chem. Phys. **90**, 6767 (1989).

[12] S. Gupta, D. C. Koopman, G. B. Westermann-Clark, and I. Bitsanis, J. Chem. Phys. **100**, 8444 (1994).

[13] D. C. Koopman, S. Gupta, R. K. Ballamudi, G. B. Westerman-Clark, and I. Bitsanis, Chem. Eng. Sci. **49**, 2907 (1994).

[14] I. Bitsanis and C. Pan, J. Chem. Phys. **99**, 5520 (1993).

[15] R. K. Ballamudi and I. A. Bitsanis, J. Chem. Phys. **105**, 7774 (1996).

[16] E. Manias, G. Hadziioannou, and G. Ten Brinke, Europhys. Lett. **33**, 371 (1996).

[17] E. Manias, G. Hadziioannou, and G. Ten Brinke, Langmuir **12**, 4587 (1996).

[18] W. E. Wallace, J. H. van Zanten, and W. L. Wu, Phys. Rev. E **52**, R3329 (1995).

[19] E. P. Giannelis, R. K. Krishnamoorti, and E. Manias, Adv. Polym. Sci. **138**, 107 (1998).

[20] R. M. Barrer and D. L. Jones, J. Chem. Soc. Inorg. Phys. Theor. A **1970**, 1531.

[21] S. Wong, R. A. Vaia, E. P. Giannelis, and D. B. Zax, Solid State Ionics **86−88**, 547 (1996).

[22] D.-K. Yang and D. B. Zax, J. Chem. Phys. **110**, 5325 (1999).

[23] R. A. Vaia, K. D. Jandt, E. J. Kramer, and E. P. Giannelis, Chem. Mater. **8**, 2628 (1996).

[24] E. Manias, E. Hackett, and E. P. Giannelis (unpublished).

[25] W. L. Mattice and U. W. Suter, *Conformational Theory of Large Molecules: The Rotational Isomeric State Model in Macromolecular Systems* (Wiley, New York, 1994); P. Robyr, Z. Gan, and U. W. Suter, Macromolecules **31**, 8918 (1998).

[26] For example: H. Sun *et al.*, COMPASS forcefield (MSI); H. Berendsen *et al.*, GRO-MACS (University of Groningen); T. R. Cuthbert, N. J. Wagner, and M. E. Paulaitis, Macromolecules **30**, 3058 (1997); R.-J. Roe, M. Mondello, H. Furuya, H.-J. Yang, *ibid.* **28**, 2807 (1995); R.-J. Roe, J. Non-Cryst. Solids **235**, 308 (1998).

[27] F. Muller-Plathe, Macromolecules **29**, 4782 (1996).

[28] E. Hackett, E. Manias, and E. P. Giannelis, J. Chem. Phys. **108**, 7410 (1998).

[29] R. A. Vaia and E. P. Giannelis, Macromolecules **30**, 7990 (1997).

[30] M. Mehring, *Principles of High Resolution NMR in Solids* (Springer, Berlin, 1983), p. 153.

[31] S. Ray, V. Ladizhansky, and S. Vega, J. Magn. Reson. **135**, 427 (1998).

[32] H. W. Spiess, Colloid Polym. Sci. **261**, 193 (1983).

[33] H. W. Spiess, J. Mol. Struct. **111**, 119 (1983).

[34] L. W. Jelinski, Annu. Rev. Mater. Sci. **15**, 359 (1985).

[35] E. Rössler, H. Sillescu, and H. W. Spiess, Polymer **26**, 203 (1985).

[36] M. Bloom, J. H. Davis, and M. I. Valic, Can. J. Phys. **58**, 1510 (1980).

[37] J. Schaefer, M. D. Sefcik, E. O. Stejskal, R. A. McKay, W. T. Dixon, and R. E. Cais, Macromolecules **17**, 1107 (1984).

[38] K. Adachi, I. Fujihara, and Y. Ishida, J. Polym. Sci., Polym. Phys. Ed. **13**, 2155 (1975).

[39] S. H. Anastasiadis, K. Karatasos, G. Vlachos, E. Manias, and E. P. Giannelis, Phys. Rev. Lett. (in press).